The 3rd International Conference on Structural Health Monitoring of Intelligent Infrastructure
Vancouver, British Columbia, Canada
November 13-16, 2007

BLAST LOAD SIMULATIONS USING HIGH RESOLUTION ANALYTICAL METHOD

Z. Yi
The City College of New York, USA

A.K. Agrawal
The City College of New York, USA

M. Ettouney
Weidlinger Associates, USA

S. Alampalli
New York State Department of Transportation, USA

Abstract

This paper presents the simulation of blast effects on a beam using a high resolution analytical method, such as finite element method with very detailed modeling. In such simulations, blast load generation, mesh size, and time step size control in the simulation determine the accuracy of results. In this paper, these aspects are discussed through comparison with experimental results.

INTRODUCTION

High resolution finite element simulation is a powerful tool to investigate effects of intentional or unintentional blast loads. It is much less expansive than experimental work and can be used to study various scenarios of blast events. However, development of a reliable model for simulation requires the complex task of blast load simulation and modeling of material behavior during high strain blast loads.

Many methods exist for evaluating structural behavior under impact loads. Closed-form wave propagation solutions usually assume a simple load distribution, neglect the elastic response and cannot be used for 3-dimensional analysis [1, 2]. Commonly used simplified methods include single or multi-degree-of-freedom, pressure-impulse (P-I) diagrams, and response surfaces developed from finite element analysis [3]. These methods have relatively low accuracy in the prediction of either load or structural performance. Li and Meng [4] have studied the loading shape effect using pressure-impulse diagram and have observed that load shape factor affects structural behavior significantly in elastic range using PI diagram method analysis. Naito and Wheaton [5] have shown that the simplified methods have to assume a proper failure type before obtaining the correct prediction. Methods with median accuracy levels include semi-empirical codes such as BlastX [6]. The most accurate results can be obtained by simulating blast loads using Hydro codes such as LS-DYNA [7] and FLEX developed by Weidlinger Associates, Inc. These hydro codes using explicit solver are designed for general purpose analysis and specific requirements must be met to obtain correct simulation results for blast effects on reinforced concrete structures. Krauthammer and Otani [8] have investigated mesh, gravity and load effects on finite element simulations of blast loaded RC concrete structures and have concluded that models with lumped reinforcements or one material type to simulate both concrete and rebar cannot capture the correct state of stress [9].

Recently, the authors have been investigating blast effects on highway bridges using high resolution finite element models. To this end, the authors have developed a finite element model of a beam subject to blast loads to correlate with one set of experimental results available. Parameters (both material and FEM) obtained from this simulation are used for simulation of a full model bridge. This paper presents finite element simulation of a beam subject to blast loads.

BLAST LOAD GENERATION

Blast wave pressure decreases rapidly with the standoff distance. Because of large size and complex geometries of a bridge structure, applying blast wave load accurately on different bridge members is a challenging work. For example, assume that a 1500-lb TNT charge is detonated under a 60-ft span hypothetical highway bridge at point C, as shown in Figure 1. The TNT charge is 10 ft away from column A and 50 ft away from column B. Pier section size is 3 ft × 3 ft.

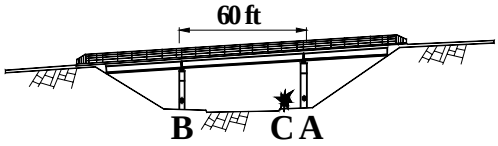

Figure 1. A hypothetical highway bridge subject to blast load.

The simulated blast wave on bridge components should at least satisfy the following:

1. Near points A and B, the pressure and impulse should be similar to that generated by experimental data or standard semi-experimental data using ConWep program [10].
2. The time of arrival of blast waves reaching point A and B should be similar to those by ConWep program so that the time sequence of blast wave load and structural response has correct dynamic effects.

Existing Approaches for Blast Load Generation

There are two traditional ways to apply blast loads on bridge components: (i) ConWep Pressure and ii) Detonation Simulation.

ConWep is a collection of conventional weapon effects calculations from the equations and curves of TM 5-855-1 [10-12]. The ConWep equation has been merged into LS-DYNA to apply a pressure load on structures [7]. This method controls load magnitude accurately and does not consume extra calculation time. However, it is only suitable for analysis before the failure of structures. When elements fail in the FEM simulation, eroding technique is used to avoid element distortion, i.e., “damaged” elements or nodes are removed from the structure. Since blast load generated by ConWep acts directly on an exposed structural surface, it will be lost once the load contact surface (i.e., exposed structural surface) is eroded. Figures 2(a) and (b) illustrate ConWep pressure directly acting on a column surface. When FEM elements in concrete cover are eroded, blast pressure is lost with erosion of these elements. On the other hand, blast load continues to act on uneroded elements. Therefore, the simulation in Figure 2(b) underestimates the damage to the structure since the load is not transmitted to concrete core.

Detonation simulation approach generates blast loads through detonation of high explosives using Arbitrary-Lagrangian-Eulerian mesh and *MAT_HIGH_EXPLOSIVE_ BURN control card in LS-DYNA. This method simulates the process of detonation and gives accurate evaluation of incident blast wave pressure through the explosive material. However, it is suitable for close range explosions [13]. As illustrated in Figures 2(c) and (d), blast pressure waves are carried to column surface using air as a medium because of standoff distance between charge and structure. This approach has several advantages over direct application ConWep pressure: (i) the blast wave load continues to act on the structure after the eroding of structural surface elements; (ii) it can predict the reflection and diffraction of the blast wave; and (iii) this method can account for the mutual interaction between structures and blast wave. This interaction cannot be ignored when the structural material yields under blast wave load with the elastic modulus approaching zero. Figure 2(d) illustrates this interaction and damage caused by blast waves. It is observed that the concrete core is damaged by simulating blast load by this approach, as opposed to only surface cover damage in case of direct ConWep loading.

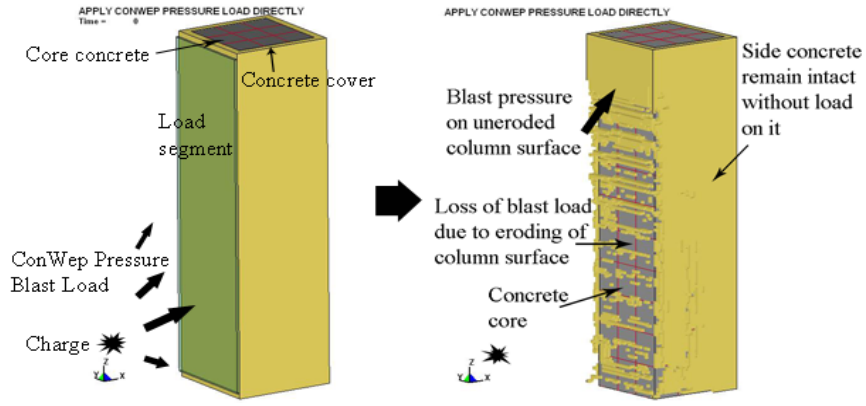

(a) ConWep generated blast load on Concrete Column. (b) Simulation results of (a)

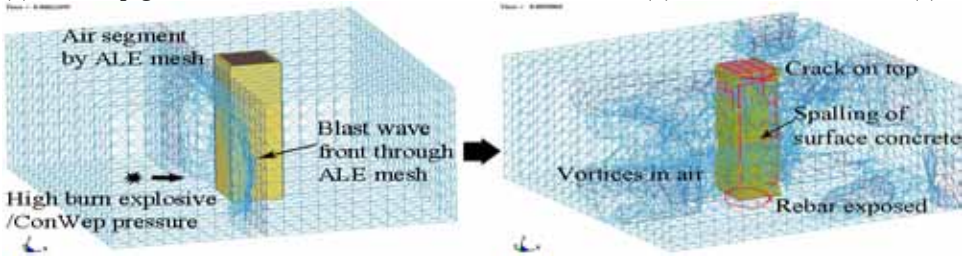

(c) Blast load generation method using Denotation. (d) Simulation of (c).

Figure 2. Blast load generation on structural elements.

Theoretically, we can simulate the reflection process by setting air mesh and reflecting boundaries using "Detonation Simulation". Problems arise when we assume air as an ideal gas, since it is difficult to simulate air under different pressure loads using simple constitutive equations. For example, blast load of 1500 lb TNT in Figure 1 is simulated using ConWep and "Detonation Simulation", as shown in Figure 3. It is observed from Figure 3 that although peak pressure generated both by ConWep and Detonation Simulation are identical, blast wave impulse (i.e., load duration) by Detonation Simulation approach is much smaller than that by ConWep, since the pressure by "Detonation Simulation" drops to zero very quickly as the standoff distance increases.

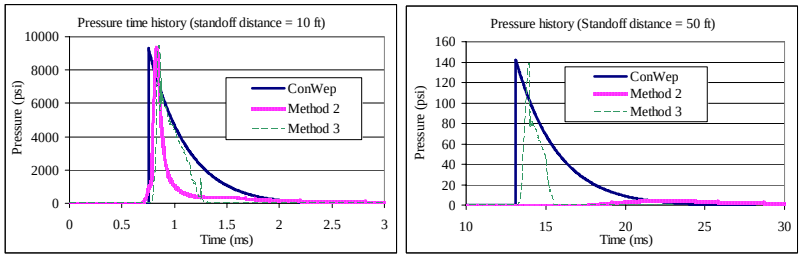

(a) Pressure at near point (b) Pressure at far point

Figure 3. Blast wave pressure history.

Proposed Approach for Blast Load Simulation

In order to overcome limitations of existing approaches, a new approach that can simulate loads on structural elements similar to ConWep is presented. In this approach, ConWep pressure generated for a specific charge weight is transferred to an air layer near structural element. The blast wave front propagates through the surrounding air layer. The blast wave front parameters include shock density, wave front air density, pressure, impulse, and time duration. However, the air density of the wave front is a key parameter to transfer the pressure correctly. Usually, the wave front air density is 2-6 times of the air density of approximately say 1.29 kg/m^3. It is found that the smaller the air density, the bigger the pressure transferred to structural elements. It has been observed from simulation results that the blast pressure is transmitted accurately to structural elements when air density of surrounding air layers is approximately twice of the normal air density value of 1.29 kg/m^3. This value is close to shock density parameter

obtained from ConWep. The air mesh interacts with Lagrangian structure element to apply the load on structural elements. This approach of applying blast loads on structural members is shown in Figures 2(c) and (d).

The proposed approach of blast load generating has advantages of both ConWep and "Detonation Simulation". It produces correct pressure field with the same arriving time of blast wave as ConWep, as seen from Fig. 3(a), and can simulate wave reflection and diffraction. When simulation involves complex geometry or non-airblast waves such as inter-explosion in box girder and air pressure near deck, other experiment data or program such as BlastX [14] is necessary to calibrate the load effect parameters.

SIMPLY SUPPORTED RC CONCRETE BEAM SIMULATIONS

In order to calibrate finite element model and determine optimal modelling parameters, experimental data on reinforced concrete beam subject to blast loading based on work by Magnusson and Hallgren (2004) has been considered [15]. Material properties and dimensions of the tested beam are presented in Table 1 and Figure 4(a). The concrete beam was assembled in a test rig, which was positioned in the test area of a shock tube (1.6m×1.2m), as shown in Figure 4(b). Table 2 shows the results obtained from air blast tests by Magnusson and Hallgren (2004).

Table 1. Properties of the beam.

Beam type	f_{cc} [1] (MPa)	Tensile reinforcement	Reinforcement ratio	f_{sy} (MPa)
B100(12)	81	4Φ12 mm	0.087	555

[1] Refers to the concrete compressive strength of $\Phi 150\times 300$ mm cylinders.

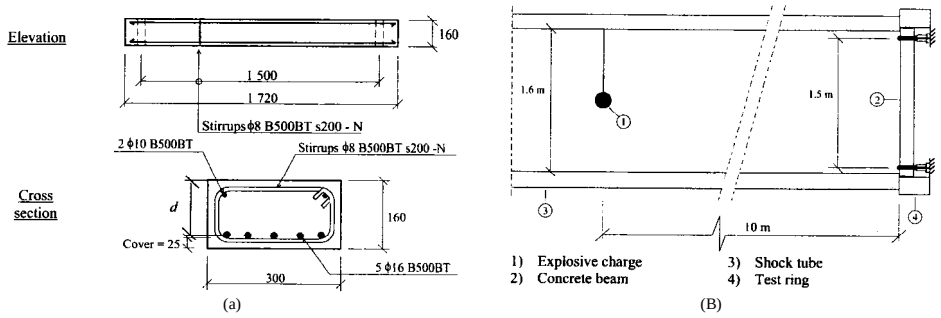

Figure 4. (a) Dimensions (in mm) of tested reinforced concrete beam; (b) Experimental set-up of the air blast tests.

Table 2. Results from the Air Blast Tests by Magnusson and Hallgren (2004).

Beam	p_r, kPa (psi)	i, kPas	$F_{tot,u}$, kN	δ_u, mm (in.)	Failure type
B100(12)-D3	1946±15 (282.2±2.2)	9.58	324	44.6 (1.756)	Flexural

In Table 2, p_r = maximum reflecting pressure (mean value ±scattering), i = impulse density (mean value ± scattering), $F_{tot,\mu}$ = maximum total support reaction and δ_u = ultimate deflection at mid-span.

Explicit solver in LS-DYNA is used for the finite element analysis. The beam model consists of 3632 solid elements, with element length approximately 1 inch. Hourglass control is applied to avoid zero energy modes. Given that the simulation time duration is short and blast pressure is very high, gravity loads are neglected in the simulation. Concrete beam is simulated by solid element with JOHNSON HOLMQUIST CONCRETE material model (MAT_111

in LS-DYNA). The Mat_111 model is capable of simulating concrete behavior during impact loads when the material experiences large strains, high strain rates and high pressures. Steel rebar is modeled as beam elements with PLASTIC KINEMATIC material (MAT_3 in LS-DYNA), assuming that perfect bond exists between concrete and rebar at the shared nodes.

Stress-strain relationship of reinforced concrete during high strain rates has been investigated extensively by several researchers recently [16-18]. It has been observed that ultimate strain values for steel and concrete are almost constant as demonstrated by many experiments and these values are selected as shown in Table 3.

Table 3. Ultimate strain Rates for concrete used in FEM simulation.

Material	Failure strain
Steel rebar	0.23
Core concrete	0.005
Cover concrete	0.002

The failure process of reinforced concrete beams with moderate percentage of steel under blast loads typically has following modes: (a) Spalling of concrete on the back of loading face; (b) Cracking of tensile concrete in the section of region with maximum moment; Failure mode is initiated by a yielding of the steel while the strains in the concrete are relatively low, with cracks climbing up to the compression region; (c) Severance of longitudinal tensile rebar; (d) Crushing of concrete in the compression region immediately after the severance of rebar. FEM model of the RC beam in Figure 5 can simulate all these stages of beam failure. As an example, the simulation figures of beam B100(12)-D3 of Table 2 are shown in Figure 5. The failure time can be taken as when the severance of longitudinal rebar occurs, as shown in Figure 5(c).

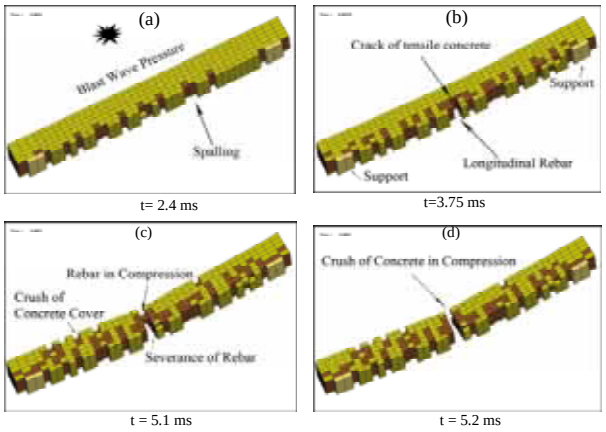

Figure 5. Failure process of beam with moderate percentage of steel

Four stages of beam damages are marked on the time-history plot of kinetic energy in Figure 6 below. A sudden rise in kinetic energy (or velocity) after state (a) is because of yielding of reinforcements. When concrete reaches its failure strain, elements are eroded and rebars are severed, resulting in loss of kinetic energy after state (d).

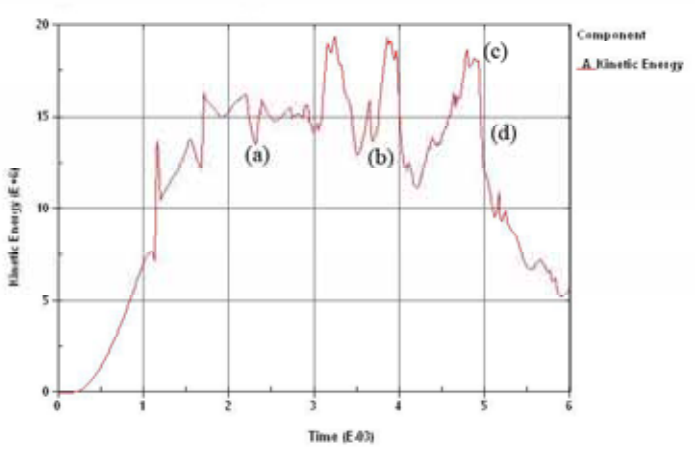

Figure 6. Kinetic energy history of concrete beam.

INFLUENCE OF MESH SIZE

In the simulation of structures with nonlinear material properties, results do not converge with mesh size due to numerical instability and is well documented in the literature. Bazant and Belytschko [19] deduced a closed-form solution to explain these difficulties. Bazant [20] showed that there existed a characteristic length for concrete material fracture. Hillerborg et al. [21] resolved these difficulties by matching the dissipation in fracture to the energy dissipated in the element which exceeds the stability threshold. In the FEM model described above, material models for concrete and steel don't have an instability problem [7]. However, when concrete and steel are combined in the FEM model, the bond slip problem is an unstable one, since the numerical model is strain-independent and is a strain-softening type because of the eroding elements (elements deleted when the failure criteria is satisfied). Although there are several approaches for modelling bond slip in numerical modeling of reinforced concrete [22-27], they all encountered difficulty in terms of stability during the blast load simulation, since eroding always involves removal of distorted elements, causing in high level of nonlinearity in the interaction between concrete and steel rebar.

In this research, the authors have extended the approach by Hillerborg et al. [21] for stability of mesh sizes to the bond slip problem. In this approach, the bond between concrete and steel is taken as a nonlinear material parameter and its dissipation energy is matched with that of the element size. It is assumed that the bond length is a characteristic length associated with concrete and steel. Therefore, the proper mesh size corresponding to the characteristic length should be determined to ensure stability of simulation.

Four FEM models of the B100 beam with different element sizes are investigated to study the influence of mesh sizes on bond slip length. Material parameters remain the same as in Table 3. The results of simulation are presented in Table 4. It is observed from Table 4 that mesh size affects the interaction between ALE air mesh and Lagrangian structure mesh significantly. Contact parameter PFAC (penalty factor) needs to be verified with experimental data to apply the correct blast pressure load on structures instead of using default values in LS-DYNA. It is observed that the midpoint deflection of the beam at failure decreases with decrease in mesh size. It is observed from Table 2 that the experimental measured value of deflection at failure is 44.6 mm (1.76 in.). This corresponds with the result of case C in Table 4. Hence, the mesh size and PFAC of case C are correct parameters for this simulation.

One interesting observation is that the reaction force varies little (less than 5%) in Table 4 while the deflection at failure varies over 400% with mesh size. This means that the calculation of transferred loads from beam to supports (e.g., columns) is stable. In other words, the response of the column can be predicted accurately if the behavior of a simply supported bridge during accidental explosion on the deck is analyzed.

Table 4. Influence of mesh size.

Case	Mesh size length (in.)	Deflection at failure (in.)	Reaction (lb)	Penalty factor PFAC	Segment Pressure (psi)
A	2.46	4.8465	-251041	0.0294	282.0
B	1.64	2.064	-230241	0.0052	282.9
C	1.08	1.756	-246334	2.06E-03	282.9
D	0.7874	1.11	-211869	4.10E-04	282.3
Test		1.756			

INFLUENCE OF TIME STEP

Table 5 presents the influence of time step on air blast pressure at the location of beam. The maximum pressure in second column of Table 4 is air pressure at the location of the beam without the beam being present. It is observed from Table 5 that the change in time step will cause a maximum of 2.59% difference in the prediction of maximum blast wave pressure.

Now, let us consider an elastic beam under blast load. Elastic material properties are used for concrete and steel in the FEM model described in Figure 5. Maximum contact pressure (pressure load transferred from ALE air mesh to Lagrangian structure mesh) in simulations with different time step control are listed in Table 6 using the Penalty factor, PFAC = 2.06E-3 corresponding to Case C in Table 4. It is observed from Table 6 that maximum contact pressure increased with decrease in time step. Hence, *contact pressure is nearly reciprocal to time step when the behavior of the beam is elastic*. PFAC factor can be adjusted to obtain the same maximum contact pressure for each case of time step in Table 6.

When the blast load is large enough to push concrete into nonlinear range, the contact mechanism is different since the interaction between air and structure is more like interaction between two fluids, i.e., the elastic modulus of structure approaches zero. *In this case, the contact pressure is relatively insensitive to both time step and penalty factor*. Consider the beam B100 beam with time steps of 4E-8 sec and 5E-8 sec with the same penalty factor (PFAC = 2.06E-3). Figure 7 shows the pressure time-history for the two cases. It is observed from Figure 7 that the peak pressures in the two cases are almost the same. Pressure attenuates faster in cases with smaller time step since numerical dissipation increases significantly with decrease in time step in the fluid solver [28]. Therefore, the largest value of constant time step, which satisfies the calculation stability requirements, can be used for simulation.

Table 5. Influence of time step to air blast load prediction.

Time Step Size (s)	Max. Pressure (psi)	Percent difference (%)
2.00E-06	196.4	0.00
1.00E-07	195.94	-0.23
5.00E-08	195.95	-0.23
1.00E-08	200.32	2.00
5.00E-09	201.48	2.59

Table 6. Contact pressure change with the time step size in elastic simulation.

Case	Time Step Size (sec)	Max. contact pressure (psi)
1	1.00E-06	328.2
2	5.00E-07	792.6
3	5.00E-08	7691
4	5.00E-09	25780

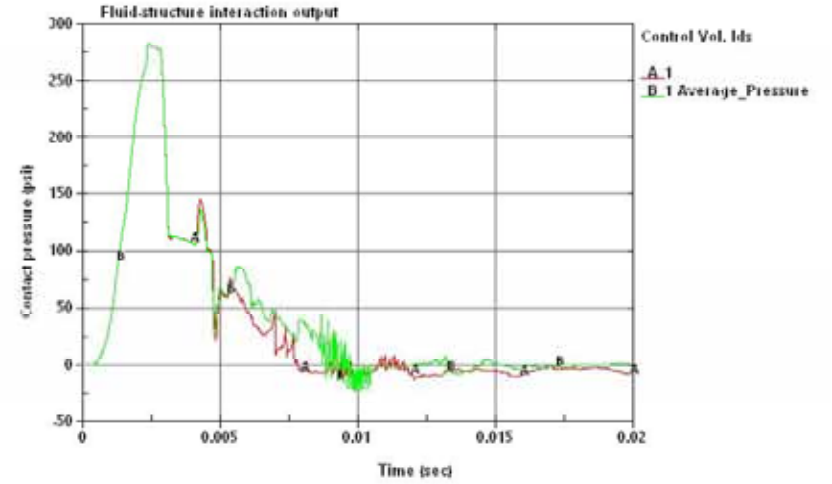

Figure 7. Contact pressure between the beam and blast wave for different time steps.

CONCLUSIONS

A new approach for simulating blast loads on structures in LS-DYNA that combines advantages of ConWep and "Detonation Simulation" is presented. The approach is successful in simulating blast loads accurately. A high resolution FEM model of a beam, calibrated using experimentally observed behavior of a beam, is developed to study penalty factors, FEM mesh size and time step required for simulation of reinforced concrete members subject to blast loads. The blast simulation with bond-slip problem and element eroding was identified as a numerical instability problem in determining mesh size. A new approach is presented to resolve this issue. For simulation of elastic structure, the change in time step caused minor difference in the prediction of maximum blast wave air pressure. In the simulation of structure with nonlinear properties, the contact pressure is relatively insensitive to both time step and penalty factor after the material yielding. Hence, a largest value of time step that satisfies stability requirements should be selected in blast simulation. These selected parameters can be used for simulation of blast effects on other components of a highway bridge model such as columns and decks.

ACKNOWLEDGMENT

This research is supported by the grants from the Multidisciplinary Center for Earthquake Engineering through Earthquake Engineering Research Centers Program of the National Science Foundation under award number EEC-9701471 and a research grant from the Region II FHWA University Transportation Research Center at the City College of New York. The views presented in this paper represent those of the authors and not necessarily of the agencies represented by the authors and sponsoring organizations.

REFERENCES

1. Jones, N., 'Structural Impact', (Cambridge: Cambridge University Press, 1989).
2. Symonds, P. S., and Mentel, T. J., 'Impulsive loading of plastic beams with axial constraint', J Mech Phys Solids 6 (1958): 186-202.
3. Sunshine, D., Amini, A., and Swanson, M., 'Overview of simplified methods and research for blast analysis'. Nashville, TN, United States: American Society of Civil Engineers, Reston, United States, 2004).
4. Li, Q. M., and Meng, H., 'Pressure-impulse diagram for blast loads based on dimensional analysis and single-degree-of-freedom model', Journal of Engineering Mechanics 128 (1) (2002): 87.
5. Naito, C. J., and Wheaton, K. P., 'Blast assessment of load-bearing reinforced concrete shear walls', Practice Periodical on Structural Design and Construction 11 (2) (2006): 112.
6. SAIC, 'BlastX Version 6.4.2.2': Science Applications International Corporation, US Army Engineer Research

and Development Center, Geotechnical and Structures laboratory and Air Force Research Laboratory, MNAL, 2006).
7. LSTC, 'LS-DYNA keyword user's manual', version 970 (Livermore: Livermore Software Technology Corporation, 2003).
8. Krauthammer, T., and Otani, R. K., 'Mesh, gravity and load effects on finite element simulations of blast loaded reinforced concrete structures', Computers and Structures 63 (6) (1997): 1113-1120.
9. Krauthammer, T., and Otani, R. K., 'Mesh, gravity and load effects on finite element simulations of blast loaded reinforced concrete structures', Computers and Structures 63 (6) (1997): 1113.
10. USAE Engineer Research & Development Center, G. S. L., 'ConWep 2.1.0.8 - Application of TM 5-855-1'. Vicksburg, MS, 2005).
11. Army, U. S. D. o. t., 'Design and analysis of hardened structures to conventional weapons effects'. Washington, DC: Headquarters, U.S. Department of the Army, 1998).
12. Hyde, D., 'ConWep 2.1.0.8 - Application of TM 5-855-1', (Vicksburg, MS, 2005).
13. Wang, J., 'Simulation of landmine explosion using LS-DYNA3D software: benchmark work of simulation of explosion in soil and air': Weapons Systems Division, Aeronautical and Maritime Research Laboratory, Australia, 2001).
14. Corporation, S. A. I., 'BlastX Version 6.4.2.2': US Army Engineer Research and Development Center, Geotechnical and Structures laboratory and Air Force Research Laboratory, MNAL, 2006).
15. Magnusson, J., and Hallgren, M., 'Reinforced high strength concrete beams subjected to air blast loading', in N. JONES, U. o. L., UK, and C.A. BREBBIA, W. I. o. T., UK, eds.(Structures Under Shock and Impact VIII. Crete, Greece, 2004).
16. Army, D. o. t., 'Structures to Resist the Effects of Accidental Explosions', (Washington, D.C.: Army Technical Manual 5-1300/Navy Publication NAVFAC P-397/Air Force Manual (AFM) 88-22 (TM 5-1300), 1990).
17. Fu, H. C., Erki, M. A., and Seckin, M., 'Review of effects of loading rate on reinforced concrete', Journal of Structural Engineering 117 (12) (1991): 3660.
18. Malvar, L. J., 'Review of static and dynamic properties of steel reinforcing bars', ACI Materials Journal 95 (5) (1998): 609.
19. Bazant, Z. P., and Belytschko, T. B., 'WAVE PROPAGATION IN A STRAIN-SOFTENING BAR: EXACT SOLUTION', Journal of Engineering Mechanics 111 (3) (1985): 381.
20. Bazant, Z. P., 'Scaling of Structural Strength', (Hermes Penton Science, London, 2002).
21. Hillerborg, A., Modeer, M., and Peterson, P., 'Analysis of crack formation and crack growth in concrete by means of fracture mechanics and finite elements', Cement Concrete Res. 6 (1976): 773-782.
22. Chen, G., and Baker, G., 'Influence of bond slip on crack spacing in numerical modeling of reinforced concrete', Journal of Structural Engineering 129 (11) (2003): 1514.
23. De Nardin, S., Almeida Filho, F. M., Oliveira Filho, J., Haach, V. G., and El Debs, A. L. H. C., 'Non-linear analisys of the bond strength behavior on the steel-concrete interface by numerical models and pull-out tests'. New York, NY, United States: American Society of Civil Engineers, Reston, VA 20191-4400, United States, 2005).
24. Limkatanyu, S., and Spacone, E., 'Reinforced concrete frame element with bond interfaces. I: Displacement-based, force-based, and mixed formulations', Journal of Structural Engineering 128 (3) (2002): 346.
25. Limkatanyu, S., and Spacone, E., 'Reinforced concrete frame element with bond interfaces. II: State determinations and numerical validation', Journal of Structural Engineering 128 (3) (2002): 356.
26. Mendola, L. L., 'Cracking Analysis of RC Members by Using Coupled BE-FE Modeling', Journal of Engineering Mechanics 123 (7) (1997): 758-761.
27. Salem, H. M., and Maekawa, K., 'Pre- and postyield finite element method simulation of bond of ribbed reinforcing bars', J. Structural Engineering 130 (4) (2004): 671.
28. Gong, M., 'Mutual Interactions between Shock Waves and Structures', Department of Engineering. New York: City University of New York, 2006).